Master Thesis
Performance Modelling and Analysis of the openQxD Lattice QCD Application

Roman Gruber

ETH Zürich, TODO:date, TODO: supervior(s)

Abstract

TODO

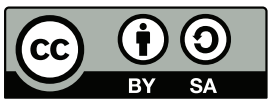

Contents

1 Introduction

TODO

In QCD blabla. orange, yellow, blue, brown, pink, red, green, purple, turquois, lightblue, lightgreen, lightpink, darkblue, lightblue , lightpink , lightgreen , linkcolor

The result of integrating $\int \sqrt{1+x}\,dx$ is given by $\frac{2(x+1)^{\frac{3}{2}}}{3}$
Python says “Hello!”

2 Conventions

3 Theory: QCD

TODO: non-abelian, hadronic physics, importance, renormalization problems, running coupling, pert theory in high enery phsyics, not in low energy regime

4 Theory: lattice QCD

TODO: as a renormalization scheme, observables, ... boundary conditions, specially SF type,

5 Theory: Performance Models

TODO: why are they important? semi-analytical, analytical vs. empritical models

6 Software: openQxD

the software package openQxD: description * importance of CG in openQxD and what it does / how it's used in the software / why 90% computation time

7 Theory: Conjugate Gradient algorithm

In many scientific computations large systems of linear equations need to be solved. Usually these systems are huge and the matrices and vectors are distributed among many ranks. The method to solve such systems should therefore be iteratively. The problem can be formulated mathematically in the following way. Let $n \in \mathbb{N}$ and let A be a $n \times n$-matrix with components in $\mathbb{C}$, hermitian, positive definite and sparse

$$\begin{aligned} A^\dagger &= A, && (\textbf{\textit{hermitian}}) \\ \forall \vec{x} \in \mathbb{C}^n \setminus \{0\} \quad : \quad \vec{x}^\dagger A \vec{x} &> 0, && (\textbf{\textit{positive definite}}) \end{aligned}$$

as well as $\vec{b} \in \mathbb{C}^n$ be given, then the ***system of linear equations*** can be described as

$$A\vec{x} = \vec{b}. \tag{7.1}$$

We are interested in the ***solution*** vector $\vec{x}$, that is the one that satisfies the above equation, n is called the ***problem size***. First let us define a function that will be helpfull in the next sections.

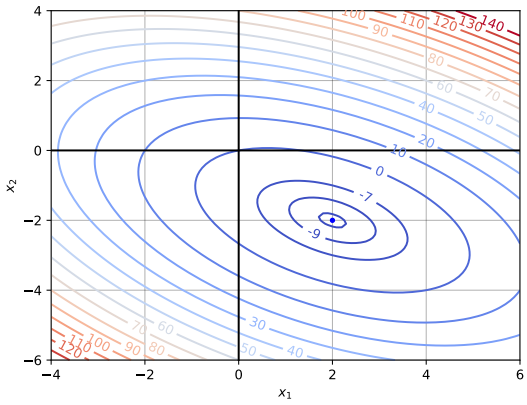

Figure 1: Quandratic form TODO

Definition 7.1 (Quadratic form)**.** *The* ***quadratic form*** *depends on the problem matrix A as well as on the* ***source*** *vector $\vec{b}$ and is defined as*

$$f(\vec{x}) = \frac{1}{2}\vec{x}^\dagger A\vec{x} - \vec{b}^\dagger\vec{x} + c,$$

where $c \in \mathbb{C}$. When taking the derivative of this function with repect to $\vec{x}$, we find that

$$f'(\vec{x}) = A\vec{x} - \vec{b}.$$

Therefore finding the extrema of $f(\vec{x})$ is equivalent to solving the linear system of equations (7.1). The question whether the solution $\vec{x}$ is unique remains.

Lemma 7.1 (Uniqueness of the solution)**.** *The solution $\vec{x}$ in equation (7.1) is unique and the global minimum of $f(\vec{x})$ if A is hermitian and positive definite* [1]*.*

Proof. Let us rewrite $f(\vec{p})$ at an arbitrary point $\vec{p} \in \mathbb{C}$ in terms of the solution vector $\vec{x}$:

$$f(\vec{p}) = f(\vec{x}) + \frac{1}{2}(\vec{p} - \vec{x})^\dagger A(\vec{p} - \vec{x}).$$

This is indeed the same as $f(\vec{p})$ (inserting $A\vec{x} = \vec{b}$ and using $A^\dagger = A$ and of $\vec{a}^\dagger\vec{b} = \vec{b}^\dagger\vec{a}$),

$$\begin{aligned} f(\vec{x}) + \frac{1}{2}(\vec{p} - \vec{x})^\dagger A(\vec{p} - \vec{x}) &= \frac{1}{2}\vec{x}^\dagger A\vec{x} - \vec{b}^\dagger\vec{x} + c + \frac{1}{2}\vec{p}^\dagger A\vec{p} - \frac{1}{2}\vec{p}^\dagger A\vec{x} - \frac{1}{2}\vec{x}^\dagger A\vec{p} + \frac{1}{2}\vec{x}^\dagger A\vec{x} \\ &= \frac{1}{2}\vec{p}^\dagger A\vec{p} + c + \vec{x}^\dagger\vec{b} - \vec{b}^\dagger\vec{x} - \vec{b}^\dagger\vec{p} \\ &= \frac{1}{2}\vec{p}^\dagger A\vec{p} - \vec{b}^\dagger\vec{p} + c \\ &= f(\vec{p}). \end{aligned}$$

In the new form of $f(\vec{p})$, one can directly see that if A is positive definite, $\vec{x}$ must minimize the function:

[1] Notice that, negative definiteness is sufficient as well and $\vec{x}$ would be the global maximum instead - just define $A' = -A$ which is positive definite and all of the argumentation that follows will hold as well. Indefinite matrices on the other hand might have local minima and maxima.

$$f(\vec{p}) = f(\vec{x}) + \frac{1}{2}\underbrace{(\vec{p}-\vec{x})^\dagger A(\vec{p}-\vec{x})}_{>0 \text{ if } A \text{ pos. def.}}.$$

Therefore $\vec{x}$ is the global unique minimum.

□

TODO: figure of a pos/neg definite quadratic form.

Before deriving the conjugate gradient method, we look at a related method called the ***method of steepest descent***. We are interested in a method that iteratively solves equation (7.1) starting at a ***initial guess*** $\vec{x}_0$ until the series is interrupted, because the approximate solution $\vec{x}_i$ might be close to the real solution by a certain tolerance or the solution was found exactly,

$$\vec{x}_0 \longrightarrow \vec{x}_1 \longrightarrow \cdots \longrightarrow \vec{x}_i \longrightarrow \vec{x}_{i+1} \longrightarrow \cdots$$

For each step, we can define the ***error*** and ***residual*** of the current step i.

Definition 7.2 (Error and Residual)**.** *Define the* ***error*** $\vec{e}_i$ *and the* ***residual*** $\vec{r}_i$ *as*

$$\vec{e}_i = \vec{x}_i - \vec{x}, \tag{7.2a}$$
$$\vec{r}_i = \vec{b} - A\vec{x}_i. \tag{7.2b}$$

The residual is the vector of dicrepancies and the same as $\vec{r}_i = -f'(\vec{x}_i) = -A\vec{e}_i$, the negative derivative of the quadratic form. The residual therefore points in direction of the steepest descent seen from the position of point $\vec{x}_i$.

Definition 7.3 (Method of Steepest Descent)**.** *The iteration step equation of the* ***method of steepest descent*** *in defined as*

$$\vec{x}_{i+1} = \vec{x}_i + \alpha_i \vec{r}_i,$$

where the $\alpha_i \in \mathbb{C}$ *are the amounts to go in direction* $\vec{r}_i$*. The* α_i *are determined by minimizing the parabola with respect to* α_i*,* $\frac{d}{d\alpha_i} f(\vec{x}_{i+1}) \stackrel{!}{=} 0$*.*

TODO: figure of steepest descent zigzac.

Remark (Convergence). As seen in figure [TODO], the method of steepest descent converges very slowly to the actual solution, when starting at a unfavorable starting point $\vec{x}_0$. The speed of convergence also heavily depends on the condition number of matrix A. We see that the iteration goes in the same direction multiple times. How about, when we only go *once* in each direction i, but by the perfect amount α_i? Then we would be done after at most n steps.

This gives motivation for a enhanced method. Let's define our new ***step equation*** as

$$\vec{x}_{i+1} = \vec{x}_i + \alpha_i \vec{d}_i, \tag{7.3}$$

with ***directions*** $\vec{d}_i$ and ***amounts*** α_i that have to be determined. But this time, we will impose the condition to go in every direction only once at most. This will lead us to the ***method of conjugate gradient***.

Using the step equation (7.3), we can update the error and residuals,

$$\vec{e}_{i+1} = \vec{x}_{i+1} - \vec{x} \tag{7.4a}$$
$$= \vec{e}_i + \alpha_i \vec{d}_i \tag{7.4b}$$
$$= \vec{e}_0 + \sum_{j=0}^{i} \alpha_j \vec{d}_j, \tag{7.4c}$$

$$\vec{r}_{i+1} = \vec{b} - A\vec{x}_{i+1} \tag{7.5a}$$
$$= \vec{r}_i - \alpha_i A\vec{d}_i \tag{7.5b}$$
$$= -A\vec{e}_{i+1}. \tag{7.5c}$$

The $\{\vec{d}_i\}$ need to form a basis of $\mathbb{C}^n$, because the method should succeed with any arbitrary initial guess $\vec{x}_0$. Since we move in the vector space $\mathbb{C}^n$ from an arbitrary point $\vec{x}_0$ to the solution $\vec{x}$, the n direction vectors need cover all possible directions in the space, therfore need to be linear independent.

To be done after at most n steps, we need that the n-th error is zero, $\vec{e}_n = 0$. Since the directions form a basis, we can write $\vec{e}_0$ as a linear combination of the $\{\vec{d}_i\}$,

$$\vec{e}_0 = \sum_{j=0}^{n-1} \delta_j \vec{d}_j.$$

Using this we can rewrite $\vec{e}_n$,

$$\begin{aligned}\vec{e}_n &= \vec{e}_o + \sum_{j=0}^{n-1} \alpha_j \vec{d}_j \\ &= \sum_{j=0}^{n-1} \delta_j \vec{d}_j + \sum_{j=0}^{n-1} \alpha_j \vec{d}_j \\ &= \sum_{j=0}^{n-1} (\delta_j + \alpha_j)\vec{d}_j.\end{aligned}$$

In order for this to be zero, all coefficients need to be zero, thus $\delta_j = -\alpha_j$. Then the i-th error can be written in a different way

$$\begin{aligned}\vec{e}_i &= \vec{e}_0 + \sum_{j=0}^{i-1} \alpha_j \vec{d}_j \\ &= \sum_{j=0}^{n-1} \delta_j \vec{d}_j - \sum_{j=0}^{i-1} \delta_j \vec{d}_j \\ &= \sum_{j=i}^{n-1} \delta_j \vec{d}_j. \end{aligned} \tag{7.6}$$

In the last row, we can see that after every step in the iteration, we shave off the contribution of one direction $\vec{d}_i$ to the initial error $\vec{e}_0$ (or phrased differently: $\vec{e}_{i+1}$ has no contribution from direction $\vec{d}_i$). But we still need to find these directions. We could for example impose that the $(i+1)$-th error should be orthogonal to the i-th direction, because we never want to go in that direction again,

$$\begin{aligned}0 &\overset{!}{=} \vec{d}_i^\dagger \vec{e}_{i+1} \\ &= \vec{d}_i^\dagger (\vec{e}_i + \alpha_i \vec{d}_i).\end{aligned}$$

This gives us a expression for the amount α_i,

$$\alpha_i = -\frac{\vec{d}_i^\dagger \vec{e}_i}{\vec{d}_i^\dagger \vec{d}_i}.$$

The problem with this expression is that we don't know the value of $\vec{e}_i$ - if we would, we could just subtract it from the current $\vec{x}_i$ and obtain $\vec{x}$ exactly. So, we do not know $\vec{e}_i$, but what we actually know is something similar, namely $-A\vec{e}_i$, with is the residual. So if we manage to samdwich an A in the expression above, we are save. It turns out that imposing A-orthogonality instead of regular orthogonality between $\vec{e}_{i+1}$ and $\vec{d}_i$ achieves what we're up to by the exact same steps,

$$\begin{aligned} 0 &\overset{!}{=} \vec{d}_i^\dagger A\vec{e}_{i+1} \\ &= \vec{d}_i^\dagger A(\vec{e}_i + \alpha_i \vec{d}_i) \end{aligned}$$

Solving for α_i gives the (almost) final expression for the amounts,

$$\implies \alpha_i = -\frac{\vec{d}_i^\dagger A\vec{e}_i}{\vec{d}_i^\dagger A\vec{d}_i} = \frac{\vec{d}_i^\dagger \vec{r}_i}{\vec{d}_i^\dagger A\vec{d}_i}. \tag{7.7}$$

Notice that the denominator is never zero, because A is positive definite. Let us continue with the expression for A-orthoginality, but insert the derived expression (7.6) for $\vec{e}_{i+1}$ this time,

$$\begin{aligned} 0 &\overset{!}{=} \vec{d}_i^\dagger A\vec{e}_{i+1} \\ &= \vec{d}_i^\dagger A \left[\sum_{j=i+1}^{n-1} \delta_j \vec{d}_j \right] \\ &= \sum_{j=i+1}^{n-1} \underbrace{\delta_j}_{\neq 0} \vec{d}_i^\dagger A\vec{d}_j. \end{aligned}$$

This implies that for $j > i$ and $i \in \{0, \dots, n-1\}$, we have

$$\vec{d}_i^\dagger A\vec{d}_j = 0.$$

But since A is hermitian, we can hermitian conjugate the whole expression above and obtain

$$0 = \left(\vec{d}_i^\dagger A\vec{d}_j\right)^\dagger = \vec{d}_j^\dagger A\vec{d}_i.$$

So the expression holds for $i > j$ as well, which implies that the $\{\vec{d}_i\}$ are ***A-orthogonal***,

$$\vec{d}_i^\dagger A\vec{d}_j = 0 \quad \forall i \neq j.$$

So the problem has reduced to finding a set of A-orthogonal vectors in an iterative way. Luckily there is a well know method to find orthogonal vectors from a set of linear independent vectors: ***Gram-Schmidt orthogonalisation***. The procedure can be altered to find A-orthogonal vectors instead.

Definition 7.4 (Gram-Schmidt Orthogonalisation)**.** *Let $\{\vec{u}_0, \dots, \vec{u}_{n-1}\} \subset \mathbb{C}^n$ be a set of n linear independent vectors. The iterative Gram-Schmidt procedure is*

$$\begin{aligned} \vec{d}_0 &= \vec{u}_0 \\ \vec{d}_i &= \vec{u}_i + \sum_{k=0}^{i-1} \beta_{ik} \vec{d}_k, \end{aligned} \tag{7.8}$$

where the $\beta_{ik} \in \mathbb{C}$ are (to be determined) coefficients. In the regluar procedure, the β_{ik} are just normalized projections of $\vec{u}_i$ to $\vec{d}_k$ that are subtracted from $\vec{u}_i$, leading to a vector $\vec{d}_i$ that is orthogonal to all previously calculated $\vec{d}_k$.

In our problem, we need a set of vectors that are A-orthogonal. By imposing this condition we find a different expression for the β_{ik},

$$\begin{aligned} 0 &\stackrel{!}{=} \vec{d}_i^\dagger A\vec{d}_j \\ &= \vec{u}_i^\dagger A\vec{d}_j + \sum_{k=0}^{i-1} \beta_{ik}\vec{d}_k^\dagger A\vec{d}_j \\ &= \vec{u}_i^\dagger A\vec{d}_j + \beta_{ij}\vec{d}_j^\dagger A\vec{d}_j, \end{aligned}$$

where in the last step, we assumed $i > j$ (else we would not find a expression for β_{ij}) and therefore only the j-th term in the sum remains, because of the A-orthonormality of the directions. Solving this for β_{ij} gives

$$\beta ij = -\frac{\vec{u}_i^\dagger A\vec{d}_j}{\vec{d}_j^\dagger A\vec{d}_j}. \tag{7.9}$$

In principle we are done here, we only need a set of linearly independent vectors $\{\vec{u}_i\}$. Since the conjugate gradient method is iterative and often dealing with huge problem sizes n, we need to store all previous directions $\vec{d}_k$ in order to calculate the current direction (see equation (7.8)). This becomes a problem in limited memory situations. We want that the current step only depends on the previous one. By imposing this condition, we need the sum in equation (7.8) to collapse; the β_{ik} should only be non-zero for $k = i-1$. If we manage to satisfy this, the orthogonalisation procedure would simplify to

$$\begin{aligned} \beta_i &\coloneqq \beta_{i,i-1}, \\ \vec{d}_i &= \vec{u}_i + \beta_i\vec{d}_{i-1}, \end{aligned}$$

where in the second equation, the current $\vec{d}_i$ only depends on the previous $\vec{d}_{i-1}$. For this to hold, all other β_{ij} need to be zero. For such a β_{ij} the numerator needs to be zero. Let therefore $j < i-1$

$$\vec{u}_i^\dagger A\vec{d}_j \stackrel{!}{=} 0.$$

To find a different expression for the left hand side, consider

$$\begin{aligned} \vec{u}_i^\dagger\vec{r}_{j+1} &= \vec{u}_i^\dagger\left(\vec{r}_j + \alpha_j A\vec{d}_j\right) \\ &= \vec{u}_i^\dagger\vec{r}_j + \alpha_j \vec{u}_i^\dagger A\vec{d}_j, \\ \implies \vec{u}_i^\dagger A\vec{d}_j &= \frac{1}{\alpha_j}\left[\vec{u}_i^\dagger\vec{r}_{j+1} - \vec{u}_i^\dagger\vec{r}_j\right], \end{aligned} \tag{7.10}$$

where we inserted the recursive relation of the resuduals (7.5b) and the yellow part is the expression we want to be zero for $j < i-1$. We therefore find a condition for the linear independent set $\{\vec{u}_i\}$, namely that the scalar product of $\vec{u}_i$ with $\vec{r}_{j+1}$ and $\vec{r}_j$ must be the same. But we can apply the same equation over and over again and obtain

$$\vec{u}_i^\dagger\vec{r}_{j+1} = \vec{u}_i^\dagger\vec{r}_j = \cdots = \vec{u}_i^\dagger\vec{r}_0, \qquad\qquad j < i-1$$

We have to find $\{\vec{u}_i\}$ that satisfy the above equation. It is sufficient to find a set of $\{\vec{u}_i\}$ that are orthogonal to all the residuals and the equation would be obeyed.

Lemma 7.2. *The residuals are orthogonal, thus for all $i \neq j$, it holds*

$$\vec{r}_i^\dagger\vec{r}_j = 0.$$

Proof. The proof consists of 2 steps.

1) Let $i < j$,

$$\begin{aligned}\vec{d}_i^\dagger \vec{r}_j &= -\vec{d}_i^\dagger A\vec{e}_j \\ &= -\sum_{k=j}^{n-1} \delta_j \vec{d}_i A\vec{d}_k \\ &= 0,\end{aligned}$$

where the yellow expression is zero, because $i < j \leq k$.

2) Let $i < j$. By step 1), we have

$$\begin{aligned}0 &= \vec{d}_i^\dagger \vec{r}_j \\ &= \vec{r}_i^\dagger \vec{r}_j + \sum_{k=0}^{i-1} \beta_{ik} \vec{d}_k^\dagger \vec{r}_j \\ &= \vec{r}_i^\dagger \vec{r}_j.\end{aligned}$$

The yellow expression is again zero by step 1). Using the symmetry of the scalar product, the above equation also holds for i and j interchanged ($i > j$), therfore holds for all $i \neq j$.

□

From now on we set $\vec{u}_i = \vec{r}_i$. What remains to find is the final expression for the β_i.

$$\begin{aligned}\beta_i \coloneqq \beta_{i,i-1} &= -\frac{\vec{u}_i^\dagger A\vec{d}_{i-1}}{\vec{d}_{i-1}^\dagger A\vec{d}_{i-1}} \\ &= -\frac{1}{\vec{d}_{i-1}^\dagger A\vec{d}_{i-1}} \frac{1}{\alpha_{i-1}} \left[\vec{r}_i^\dagger \vec{r}_i - \vec{r}_i^\dagger \vec{r}_{i-1}\right] \\ &= -\frac{\vec{r}_i^\dagger \vec{r}_i}{\alpha_{i-1}\vec{d}_{i-1}^\dagger A\vec{d}_{i-1}} \\ &= -\frac{\vec{r}_i^\dagger \vec{r}_i}{\vec{d}_{i-1}^\dagger \vec{r}_{i-1}},\end{aligned}$$

where in the first row we used the definition (7.9), in the second row we have used equation (7.10) and the yellow expression is zero by the orthogonality of the residuals lemma 7.2. In the last line we used the expression for the α_j equation (7.7)

To obtain the final form of the α_i and the β_i, we can use a leftover of the proof of lemma 7.2, namely

$$\begin{aligned}\vec{d}_i^\dagger \vec{r}_i &= \vec{r}_i^\dagger \vec{r}_i + \beta_i \underbrace{\vec{d}_{i-1}^\dagger \vec{r}_i}_{=0 \text{ by lemma 7.2 step 1)}} \\ &= \vec{r}_i^\dagger \vec{r}_i.\end{aligned}$$

Using this we find the final form of the α_i and the β_i as well as the ***method of conjugate gradient***.

Definition 7.5 (Method of conjugate gradient)**.** *The iteration step equation of the* ***method of conjugate gradient*** *in defined as*

$$\vec{x}_{i+1} = \vec{x}_i + \alpha_i \vec{d}_i,$$

with

$$\vec{d}_{i+1} = \vec{r}_{i+1} + \beta_{i+1}\vec{d}_i, \qquad \alpha_i = \frac{\vec{r}_i^\dagger \vec{r}_i}{\vec{d}_i^\dagger A\vec{d}_i}, \tag{7.11}$$

$$\vec{r}_{i+1} = \vec{r}_i - \alpha_i A\vec{d}_i, \qquad \beta_{i+1} = -\frac{\vec{r}_{i+1}^\dagger \vec{r}_{i+1}}{\vec{r}_i^\dagger \vec{r}_i}, \tag{7.12}$$

and initial starting vectors

$$\vec{x}_0 = \textit{arbitrary starting point},$$
$$\vec{d}_0 = \vec{r}_0 = \vec{b} - A\vec{x}_0.$$

There are some remarks to note about the method of conjugate gradient.

Remark. The β_{i+1} of the current iteration depends on the norm of the current residual as well as the last one. This means that we can store the result of the last iteration and reuse it in the current, the norm may not be calculated twice.

Remark. In the souce code of openQxD (see [2]) the matrix A is the Dirac matrix applied twice $A = D^\dagger D$. This means that the denominator of α_i is a regular inner product as well; $\vec{d}_i^\dagger A\vec{d}_i = \vec{d}_i^\dagger D^\dagger D\vec{d}_i = \left(D\vec{d}_i\right)^\dagger \left(D\vec{d}_i\right) = \left\|D\vec{d}_i\right\|^2$

Remark. Therefore in each iteration, we have:

- 2 times the norm of a vector,
- 2 matrix-vector multiplications,
- 3 times axpy.[2]

Remark (Floating point errors). Since the method contains recursive steps, floating point roundoff accumulation is an issue. This causes the residuals to loose their A-orthogonality. It can be resolved by calculating the residual from time to time using its (computationally more expensive) definition $\vec{r}_i = \vec{b} - A\vec{x}_i$, which involves one matrix vector multiplication. One can for example do this every m-th step. The same problem applies to the directions $\vec{d}_i$ that loose their A-orthogonality.

Remark (Problem size). The method of conjugate gradient is suitable for problems of very huge size n. The algorithm is done after n steps, but there might be problems such that even n steps are out of reach for an exact solution.

Remark (Time complexity). The time complexity of the conjugate gradient method is $O(m\sqrt{\kappa})$, where m is the number of non-zero entries in A and κ is its ***condition number***.

Remark (Starting). The ***starting vector*** $\vec{x}_0$ can be chosen at wish. If there is already a rough estimate of the solution one can take that vector. But usually just $\vec{x}_0 = 0$ is chosen. Since the minimum is global, there is no issue in chosing a starting point. The method will always converge towards the real solution.

Remark (Stopping). If the problem size does not allow to run n steps, one can stop when the norm of the residual falls below a certain ***threshold*** value. Usually this threshold is a fraction of the initial residual $\|\vec{r}_i\| < \epsilon\|\vec{r}_0\|$ [11].

[2] This stands for $a\vec{x} + \vec{y}$, scalar times vector plus vector, "a x plus y" (to resemble the BLAS level 1 routine call of the same name).

8 Theory: Real number formats

8.1 IEEE Standard for Floating-Point Arithmetic

Floating point numbers are omnipresent in the scientific applications. In the conjugate gradient kernel of [2], there are large scalar products over vectors of very high dimensionality over multiple ranks. The components of these vectors are single precision floating point numbers (I call them binary32 from here on). The precision was degraded from binary64 to binary32 already and a speedup of a factor of 2 was achieved. This motivates to explore even smaller floating point formats with encoding lengths of 16 bits. Since scalar products as well as matrix-vector products are memory-bound operations, going to a smaller bit-length will increase the throughput of the calculation. Therefore, a 16 bits floating point format with a smaller exponent could lead to a double of performance if the new operation is still memory-bound.

Definition 8.1 (IEEE 754 Floating point format)**.** *The **IEEE 754 floating point format** [8] is defined using the **number of exponent bits** e and the **number of mantissa bits** m respectivetly. A binary floating point number is illustrated in figure 2.*

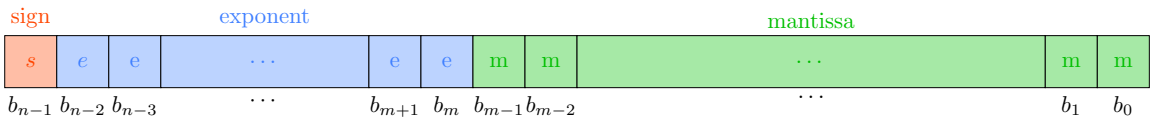

Figure 2: Binary representation of a IEEE 754 n-bit precision floating-point number. The orange bit represents the sign bit, the blue bits represent the fixed-length e exponent bits and the green bits represent the fixed-length m mantissa bits. Notice that $n = 1 + e + m$.

The resulting floating point number is then calculated as

$$f = (-1)^s \cdot M \cdot 2^E,$$

where $E = E' - B$ denotes the biased exponent, B is the exponent bias, M the mantissa and s the sign bit. The (unbiased) exponent E' is calculated as follows

$$E' = \sum_{i=0}^{(e-1)} b_{m+i} 2^i, \tag{8.1}$$

where B is the exponent bias.

Definition 8.2 (Exponent bias)**.**

$$B = 2^{(e-1)} - 1,$$

The calculation of the mantissa is a bit more involved, since it depends on the number being normal or subnormal.

Definition 8.3 (Subnormal numbers)**.** *The IEEE 754 standard introduces so called **subnormal numbers**. If all the exponent bits are* 0*, meaning the unbiased exponent $E' = 0$, and the mantissa bits are not all* 0*, then the number is called subnormal. The exponent being zero causes the implcit bit to flip to* 0*, instead of* 1*.*

Remark. Subnormal numbers have a variable-length mantissa and exponent, because some of the mantissa bits are used as additional exponent bits, making the numbers less precise the lower they get (see the smooth cutoff in figure 4).

Therefore the mantissa of a regular (non-subnormal) number is (when the exponent $0 < E < B$, this implies that the implicit bit is 1)

Floating point formats				
name	s	e	m	comment
binary64	1	11	52	double precision, IEEE 754 [9]
binary32	1	8	23	single precision, IEEE 754 [9]
binary16	1	5	10	half precision, IEEE 754 [9]
bfloat16	1	8	7	Googles Brain Float [12]
tensorfloat32	1	8	10	NVIDIAs TensorFloat-32 [7] [3]
binary24	1	7	16	AMDs fp24 [1]
binary128	1	15	112	IEEE 754 [9]
binary256	1	19	236	IEEE 754 [9]

Table 1: Commonly used floating point formats, where s is the number of sign bits, e the number of exponent bits and m the number of mantissa bits.

$$M = \underset{\text{implicit bit}}{1} + \sum_{i=1}^{m} b_{m-i} 2^{-i},$$

whereas the mantissa of a subnormal number (when the exponent $E = 0$) is

$$M = \underset{\text{implicit bit}}{0} + \sum_{i=1}^{m} b_{m-i} 2^{-i},$$

The 1 or 0 in the front of the summand is the leading ***implicit bit***, sometimes also called the $(m+1)$***-th mantissa bit*** that tells us whether the number is subnormal or not.

Remark. The mantissa range of a regular floating point number is $M \in [1, 2)$, whereas the matissa range of a subnormal floating point number is $M \in (0, 1)$. The number zero is not considered subnormal.

Usual floating point formats are summarised in table 1.

The format of interest is the binary16 half precision IEEE 754 floating point format. The highest representable number is when the exponent is highest. This is not the case when all e exponent bits are 1, because then - according to the specification [8] - the number is either $\pm\infty$ or not a number (NaN), depending on the mantissa. The maximal unbiased exponent is therefore the next smaller number,

$$E'_{max} = \underbrace{1 \ldots 1}_{e-1 \text{ times}} 0.$$

Using equation (8.1), we find

$$\begin{aligned} E'_{max} &= \sum_{i=1}^{(e-1)} 2^i \\ &= 2^e - 2. \end{aligned}$$

The mantissa on the other hand is maximal when all mantissa bits are 1 (including the implicit bit),

$$M_{max} = 1 + \sum_{i=1}^{m} 2^{-i}$$

[3] Allocates 32 bits, but only 19 bits are actually used.

Floating point format limits				
name	f_{max}	f_{min}	f_{smin}	sign. digits [4]
binary64	1.8×10^{308}	2.2×10^{-308}	4.9×10^{-324}	≤ 15.9
binary32	3.4×10^{38}	1.2×10^{-38}	1.4×10^{-45}	≤ 7.2
binary16	6.6×10^{4}	6.1×10^{-5}	6.0×10^{-8}	≤ 3.3
bfloat16	3.4×10^{38}	1.2×10^{-38}	9.2×10^{-41}	≤ 2.4
tensorfloat32	3.4×10^{38}	1.2×10^{-38}	1.1×10^{-41}	≤ 7.2
binary24	1.8×10^{19}	2.2×10^{-19}	3.3×10^{-24}	≤ 5.1
binary128	1.2×10^{4932}	3.4×10^{-4932}	6.5×10^{-4966}	≤ 34
binary256	$1.6 \times 10^{78,913}$	$1 \times 10^{-78,912}$	$1 \times 10^{-78,983}$	≤ 71.3

Table 2: Summary of highest representable numbers, minimal subnormal and non-subnormal representable numbers above 0 in any IEEE 754 floating point format together with their approximated precision.

$$= 2 - 2^{-m}.$$

Using these two formulas we can define the

Definition 8.4 (***highest representable number***)**.** *The* ***highest representable number*** *in any floating point format is*

$$\begin{aligned} f_{max} &= (-1)^0 \cdot M_{max} \cdot 2^{(E'_{max}-B)} \\ &= (2 - 2^{-m}) \cdot 2^{(2^e - 2^{e-1} - 1)} \\ &= (2 - 2^{-m}) \cdot 2^{(2^{e-1}-1)}. \end{aligned}$$

The minimal number above 0 can be found similarly, using minimal unbiased exponent (when all exponent bits are 0, except the last one, therefore $E'_{min} = 1$) and the minimal mantissa ($M_{min} = 1$).

Definition 8.5 (***minimal (non-subnormal) representable number above*** 0)**.** *The* ***minimal (non-subnormal) representable number above*** 0 *in any floating point format is*

$$\begin{aligned} f_{min} &= (-1)^0 \cdot M_{min} \cdot 2^{(E'_{min}-B)} \\ &= 2^{(2-2^{e-1})}. \end{aligned}$$

The minimal subnormal number can the found, when the unbiased exponent consists of only zeros ($E'_{smin} = 0$) and for the mantissa, only the rightmost bit is one ($M_{smin} = 2^{1-m}$).

Definition 8.6 (***minimal subnormal representable number above*** 0)**.** *The* ***minimal subnormal representable number above*** 0 *in any floating point format is*

$$\begin{aligned} f_{min} &= (-1)^0 \cdot M_{smin} \cdot 2^{(E'_{smin}-B)} \\ &= 2^{1-m} \cdot 2^{(1-2^{e-1})} \\ &= 2^{(2-m-2^{e-1})}. \end{aligned}$$

See table 2 for these limiting numbers in the different floating point formats.

8.2 Posits

The posit datatype is designed to be a replacement for the IEEE floating point format, fixing its various quirks. Some of the more entertaining are:

[4] Number of significant digits in decimal; $-\log_{10}(\texttt{MACHINE\_EPSILON}) = \log_{10}(2^{m+1})$.

- The appearance of NaNs. They are considered unnatural, because a specific bit pattern describing a number that is not a number is a contradiction.
- The NaNs and the fact that floats have two different representations for the number zero (0 and -0) lead to very complicated and slow comparison units.
- Floats may under- or overflow, because the standard employs the round to nearest even rounding rule ($\pm\infty$ and 0 are considered even).
- Floats are non-associative and non-distributive[5]leading to rounding errors that have to be taken into account, specially in scientific computing.
- The standard gives no guarantee of bit-identical results across systems.

The goal is to utilise the number of bits more efficiently and remove these inconsistencies. The key idea is to place half of all numbers between 0 and 1 and the other half are the reciprocals (the reciprocal of 0 being $\pm\infty$). The number can then be drawn on a projective real number circle [6]. The structure of a binary posit number is illustrated in figure 3.

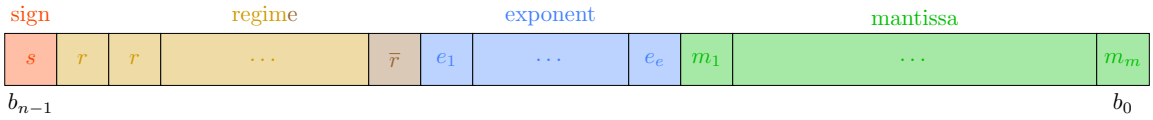

Figure 3: Binary representation of a n-bit posit number. As with regular floats the orange bit represents the sign bit, the yellow bit(s) represent the variable length regime bit(s) terminated by the brown bit that is the opposite regime bit, the blue bit(s) represent the variable-length exponent bit(s) and the green bit(s) represent the variable-length mantissa bit(s).

The actual value of the number is calculated as follows. The yellow and brown bits determine the regime of the number. They either start with a row of all 0 or all 1 terminated by the opposite bit indicating the end of the row. The number of bits in the row are counted as m and if they are all 0 they get a minus sign, the regime being $k = -m$. If they are all 1 the regime is calculated as $k = m - 1$. After the regime is decocded, the remaining bits contain the exponent with at most es bits depending on how much bits remain. If no bits remain the exponent is 0. The exponent and the mantissa are both of variable length. Both can have 0 bits, in this case the number consists of only regime bits. This is the reason why posits have a larger number range than floats. The exponent is enconded as unsigned integer, so there is no bias and no bit pattern denoting special numbers such as subnormals or NaNs. Therefore n-bit posits have more numbers than n-bit floats, because they have no NaNs. After the exponent - if there are still bits remaining - the fraction follows, else the fraction is just 1.0 Since there are no subnormals the implicit bit is always 1. There are two special numbers that do not follow the above encoding scheme; zero which has the bit pattern of all 0 and $\pm\infty$ with a 1 followed by all 0. These two numbers are reciprocals of each other. A general posit number can therefore be written as

$$p = (-1)^s \cdot useed^k \cdot M \cdot 2^E,$$

where s is the sign bit, $useed$ is defined to be $useed = 2^{2^{es}}$, with es the number of predefined exponent bits, M is the mantissa and E the exponent.

The mantissa is calculated as

$$M = 1 + \sum_{i=1}^{m} m_i 2^{m-i},$$

where m is the variable number of mantissa bits and the implicit bit in front of the sum is always 1. The exponent is

[5]There was even a system using IEEE 754 that had non-commutative floating point operations[3].

Posit format limits				
name	*es*	p_{max}	p_{min}	sign. digits [6]
posit64	3	2.0×10^{149}	4.9×10^{-150}	≤ 17.7
posit32	2	1.3×10^{36}	7.5×10^{-37}	≤ 8.1
posit16	1	2.7×10^{8}	3.7×10^{-9}	≤ 3.6
posit8	0	64	1.6×10^{-2}	≤ 1.5

Table 3: Summary of highest representable numbers, minimal representable numbers above 0 in any posit format together with their approximated precision.

$$E = \sum_{i=1}^{e} e_i 2^{e-i},$$

where e is the variable number of exponent bits satisfying $e \leq es$.

Using these two equations, we are now able to calculate the highest representable number and the minimal representable number above 0 in posit format.

Definition 8.7 (***highest representable number***)**.** *The* ***highest representable number*** *in any posit format is*

$$\begin{aligned} p_{max} &= (-1)^0 \cdot useed^{n-2} \\ &= 2^{2^{es}(n-2)}. \end{aligned}$$

Definition 8.8 (***minimal representable number above*** 0)**.** *The* ***minimal representable number above*** 0 *in any posit format is the reciprocal of the highest representable number* p_{max}

$$\begin{aligned} p_{min} &= \frac{1}{p_{max}} \\ &= 2^{2^{es}(2-n)}. \end{aligned}$$

See table 3 for these limiting numbers in the different posit formats.

Posits employ a feature called the quire, which is the generalized answer to the fused multiply–add operation that recently found its way into [9] in 2008, where the rounding is deferred to the very end of the operation.

8.3 Floating point numbers in openQxD

To explore how the conjugate gradient kernel in openQxD would perform when using smaller bit lengths, one can look at the exponentials of the numbers in the matrix and vectors, see figure 5. The plot shows all exponents appearing together with their overall occurence in percent. The number zero was taken from the plot, because it has biased exponent $E = -127$. The occurences for zero are given in the legend.

The highest exponent in all 4 runs was $E = 4$, whereas the lowest exponent deceased when the number of lattice points increased. The range of exponents that is representable in binary16 spans from -24 to $+16$ and is indicated by the solid orange line and the solid pink line. Between -24 and -14 is the regime of subnormal numbers in binary16, with the lowest regular (non-subnormal) exponent indicated by the solid blue line. When using half precision instead of single precision, all numbers with exponents below -24, will be converted to zero, whereas exponents above $+16$ will be casted to $\pm\infty$ depending on the sign of the number. It can be seen, that when calculating the

[6] Number of significant digits in decimal; $-\log_{10}$(`MACHINE_EPSILON`). Notice that posits have ***tapered accuracy***; numbers near 1 have much more precision than numbers at the borders of the regime. The precision of floats decreses as well with very large and small numbers, but posit precision decreases faster, see figure 4.

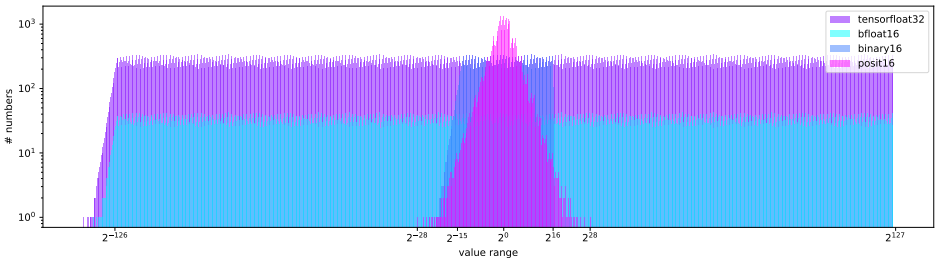

Figure 4: Density or distribution of numbers for tensorfloat32, binary16, posit16 and bfloat16. The number of bins was chosen to be 1024 of logarithmic width. The IEEE conformant floats tensorfloat32, binary16 and bfloat16 exhibit a simmilar shape, namely the distribution of numbers is exponential decreasing for higher and smaller numbers. The high numbers undergo a rough cutoff at the highest representable number. Numbers above that value will be cast to infinity. Compared to this, the small numbers show a smooth cutoff, because of the existence subnormal numbers. The range of posit16 is bigger than the range of binary16, but specially in the very small numbers this difference in range is neglectible. Some features of posits can be observed: First, their distribution is symmetric around 1, because posits have no subnormals. Second, more numbers are closer to 1 than in case of floats; the closer to 1, the better the number resolution. Closest to 1, the number resolution becomes better than binary16 resolution. Third, posits have no fixed-length mantissa nor exponent. That's the reason why the height of the posit shape depends on the number regime, which happens for floats only in the subnormal regime, where the exponent and mantissa are indeed of variable length. For all formats, the amount of numbers decreases exponentially when going away from 1, but posits decrease faster. This suggests that when calculating in the number regime close to 1 posits might be the better choice, but when numbers span the whole number range equally, floats might be superior. But in that case one has to take care about over- and underflows. Notice that the height of the shape is determined by the number of mantissa bits, therefore giving the precision, whereas the width is determined by the number of exponent bits, therefore giving the number range. For example tensorfloat32 and binary16 have a very different number range, but exhibit the same percision for numbers in their intersection, meaning that binary16 is a subset of tensorfloat32. On the other hand comparing tensorfloat32 and bfloat16 they have approximately the same number range, but different precisions in them, meaning that bfloat16 is as well a subset of tensorfloat32, which itself is a subset of binary32. Notice that when plotting binary32 and posit32 in such a plot, they would look very similar to binary16 versus posit16.

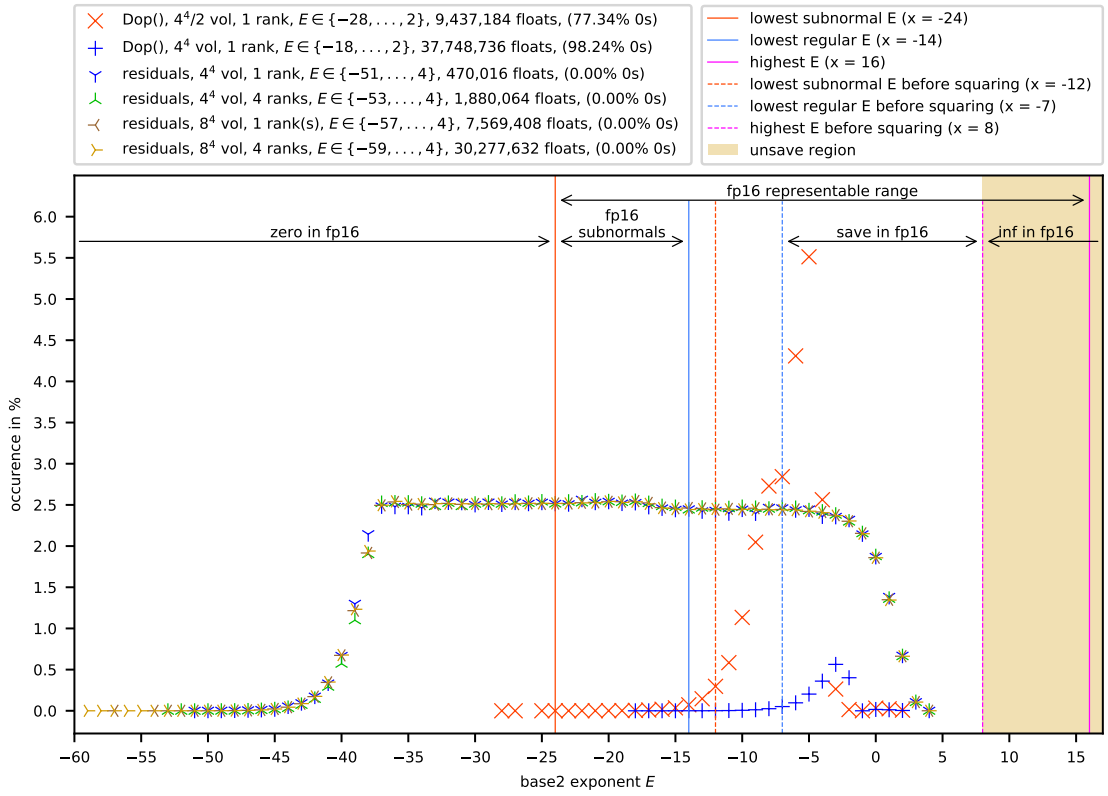

Figure 5: Exponent distribution of binary32 single precision floats in the residual vectors of all steps in a conjugate gradient run in openQxD as well as entries of the Dirac operator. 4 runs were made, with a lattice size of 4^4 and 8^4 on one single rank and 4 ranks respectively. The number is normalised to $(-1)^s \cdot M \cdot 2^E$, where $M \in [1, 2)$.

norm of these numbers, only numbers between the dashed blue line and the dashed pink line will participate. If there is a number above the dashed pink line in the unsave region this number will - after squaring - be casted to ∞ and therefore the norm will be ∞ as well[7]. In this case the variable representing the norm $x = \|\vec{v}\|$ should be of higher precision than binary16. The plot shows that the Dirac matrix `Dop()` is confined in a narrow exponent regime and a representation in 16-bit floats would suffice. Notice the sparsity the Dirac matrix.

8.4 The conjugate gradient kernel

The conjugate gradient kernel `cgne()` in `modules/linsolv/cgne.c` in [2] implements the algorithm. The function expects the Dirac matrix `Dop()` in binary32, `Dop_dble()` in binary64 format and the source vector `eta` ($\vec{b}$) in binary64 only. In the initialisation the starting vector `psi` ($\vec{x}_0$) is set to zero. The algorithm stops when the desired maximal relative residue `res` ($= \frac{\|\texttt{eta} - D^\dagger D \texttt{psi}\|}{\|\texttt{eta}\|}$) is reached, where `psi` is the calculated approximate solution of the Dirac equation $D^\dagger D$`psi` = `eta` in binary64. For this, the tolerance `tol` is calculated using `tol` = $\|$`eta`$\| *$`res`. The parameter `nmx` is the maximal number of iterations that may be applied and `status` reports the total number of iterations that were required, or a negative value if the algorithm failed. Since the Dirac matrix is given in two precisions, the algorithm in the code bails out of the main loop, when some particular conditions where met, see listing 1.

This may happen in 4 cases:

[7] A method to circumvent this is to scale the vector entries during the calculation and scale the result back, exploiting homogeneity of the norm, $\|\vec{v}\| = \frac{1}{s}\|s\vec{v}\|$ for $s \in \mathbb{R}_{>0}$.

```
490 if ((rn<=tol)||(rn<=(PRECISION_LIMIT*xn))||(ncg>=100)||
491     ((*status)>=nmx))
492   break;
```

Listing 1: break condition in `modules/linsolv/cgne.c` line 490ff, `rn` is the norm of the current residual, `xn` is the norm of the current solution vector, both in binary32.

1. if the recusively calculated residual is below the tolerace,
2. if the precision of binary32 is reached[8],
3. after a hardcoded number of 100 steps,
4. if the maximal number of steps is reached.

Point 2 is the most interesting condition, because lets imagine that this condition is met, but the algorithm does not break out of the main loop. Therefore the norm of the current residual compared to the norm of the current solution vector differ in their orders of magnitude by the precision limit of the datatype (binary32 in this case). This means that the solution vector $\vec{x_i}$ contains large numbers compared to the residual vector $\vec{r_i}$. Therefore the changing in residual from iteration to iteration is small compared to numbers in $\vec{x_i}$ as well. Since $\vec{r_i}$ contains small numbers, the amounts α_i are small as well. This causes $\vec{x_{i+1}} = \vec{x_i} + \alpha_i \vec{d_i}$ to not change anymore, because adding very large and very small numbers in floating point arithmetic will return the larger number unchanged if the two numbers differ by the precision limit of the datatype. The algorithm stalls in that case and breaking out of the main loop is the emergency brake.

So when one of the above conditions are met, the algorithm performs a ***reset step***. A reset step consists of calculating the residual not in the recursive way, instead calculating it as it's definition $\vec{r_i} = \vec{b} - A\vec{x_i}$ in double precision. This involves 2 invocations of each `Dop_dble()` as well as `Dop()` which is very expensive. The algorithm is resetting in the sense that the solution vector is set back to $\vec{x_i} = 0$, but before resetting, the solution vector in binary32 is added to the real solution vector `psi` in binary64 which was initialied to zero at the start of the algorithm. It looks like a restart of the whole calculation, but the direction for the next iteration $\vec{d_i} = \vec{r_i}$ is set to the just calculated, very accurate residual, therefore the the algorithm now continues in a new direction A-orthogonal to all previous directions and progression is kept. The step is meant to remove the accumulated roundoff errors due to the recursive calcuation of the residuals and directions. The less precise the datatype, the more reset steps need to be taken, because the precision limit is reached earlier.

8.5 Simulating other datatypes

Some operations such as norms and scalar products are memory-bandwidth-bound, which means the on-chip memory bandwidth determines how much time is spent computing the output. Storing input data in a format with lower bit-length reduces the amount of data to be transferred, thus improving the speed of calculation.

The complete conjugate gradient kernel was simulated in different datatypes, floats as well as posits. In order to produce the plots, the dirac matrix `Dop_dble()` and the source vector `eta` were extracted in binary64 format from the original code with a simulation of a 4^4 lattice, periodic boundary conditions (`type 3`), no C* boundary conditions (`cstar 0`) and 1 rank. A python script mimicking the exact behavior of the `cgne()` function from the source code[9], was implemented to cope with arbitrary datatypes. The simulated datatypes were binary64, binary32, tensorfloat32, binary16, bfloat16, posit32, posit16, and posit8. The Dirac matrix had 2% non-zero value. The results are plotted in figures 6, 7, 8 and 9.

[8] The constant `PRECISION_LIMIT` is defined to be `100*MACHINE_EPSILON`, where the `MACHINE_EPSILON` is the difference between 1 and the lowest value above 1 depending on the datatype. In case of binary32 the `MACHINE_EPSILON` takes a value of $1.192{,}092{,}9 \times 10^{-7}$.

[9] See line 429ff in `modules/linsolv/cgne.c` in [2].

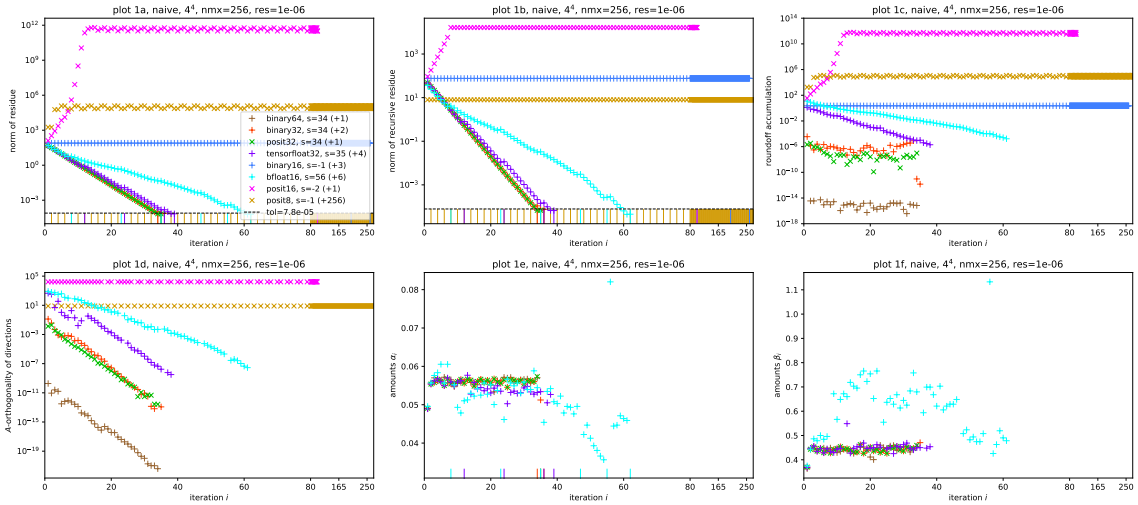

Figure 6: Convergence analysis of a conjugate gradient run, where binary32 was replaced by one of the simulated datatypes. The number `s` describes the number of normal steps needed (the value of `status`), whereas the numbers in the brackets indicates the number of reset steps. All reset steps are indicated by ticks at the dashed black tolerance line. The iterations will always go up to `nmx=256`, but the range 80-256 is compressed since the most interesting behavior happens before step 80 for most of the simulated datatypes. The 4 plots show the naive replacement of the binary32 datatype with the simulated one. This means that every single variable containing a binary32 was replaced with a variable of the simulated datatype. Plot *1a* shows the exact residue (7.5a) in every iteration calculated using the Dirac matrix and the source vector both in binary64, whereas plot *1b* shows the norm of the recursively calculated residue (7.5b) (casted after the calculation from the simulated datatype to binary64). The relative residue suffers roundoff accumulation because of the recusive calculation; this is the differnce between plots *1a* and *1b*, which is plotted in plot *1c*. Plot *1d* shows the A-orthogonality of the current direction to the last direction, namely the value of $\vec{d}_i^{\dagger} A \vec{d}_{i+1}$. The last 2 plots, *1e* and *1f*, show the values of the amounts α_i and β_i (see equations (7.11) and (7.12)) in every iteration, only of the datatypes that converged (`status>0`).

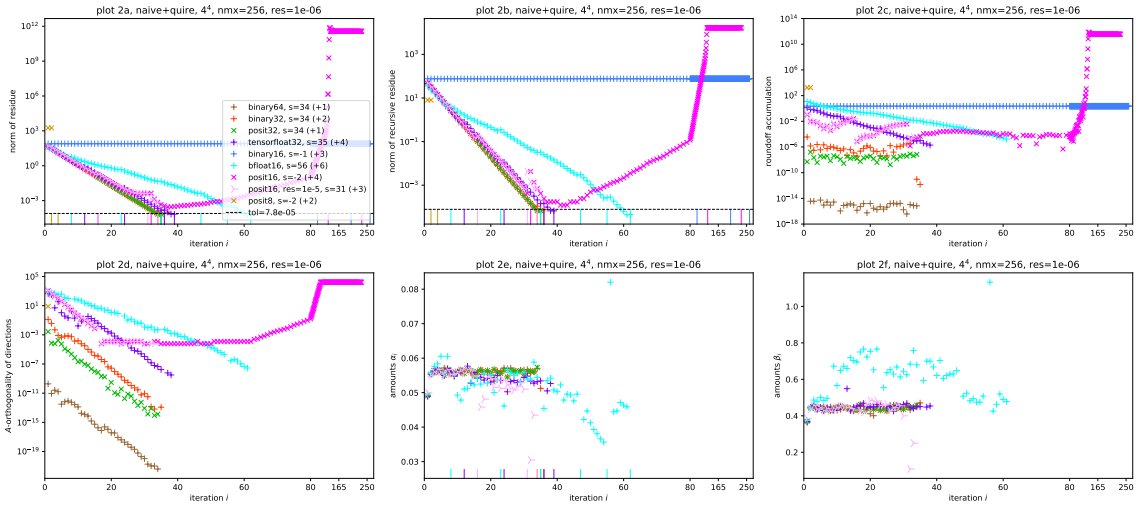

Figure 7: In these plots, the posits were utilizing quires as their collective variables, the remaining setup was the same as for firgure 6, therefore the floating point datatypes show exactly the same values, only posits changed their behavior.

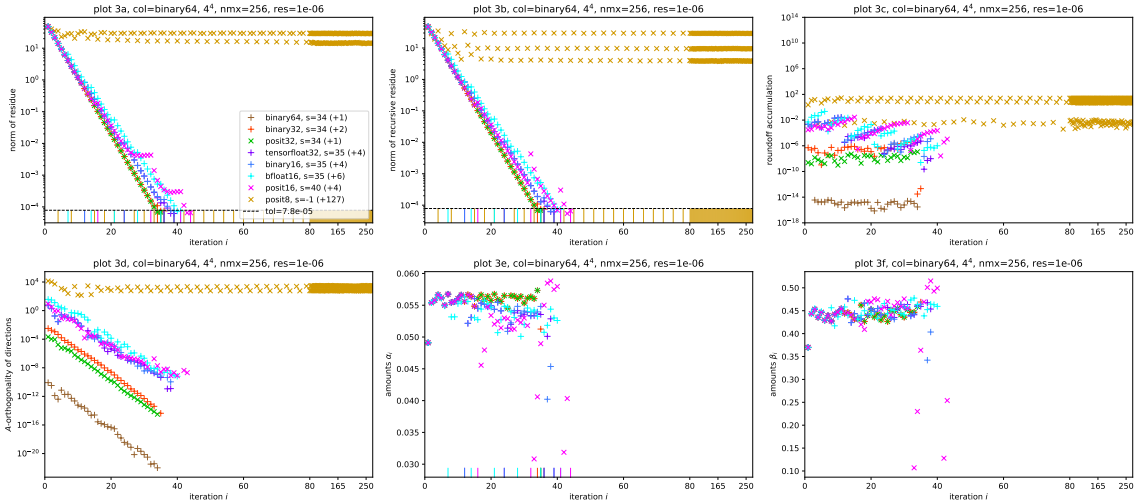

Figure 8: The 4 plots introduce a slightly smarter replacement. All collective variables such as norms where calculated in binary64, such that a datatype with a small number range such as binary16 may not over- or underflow when calculating the norm of a vector full of said datatype. This replacement resembles the quire for posits. Using this replacement, even heavily reduced datatypes like binary16 and posit16 converged and threw a result of equal quality as the one simulated with binary64.

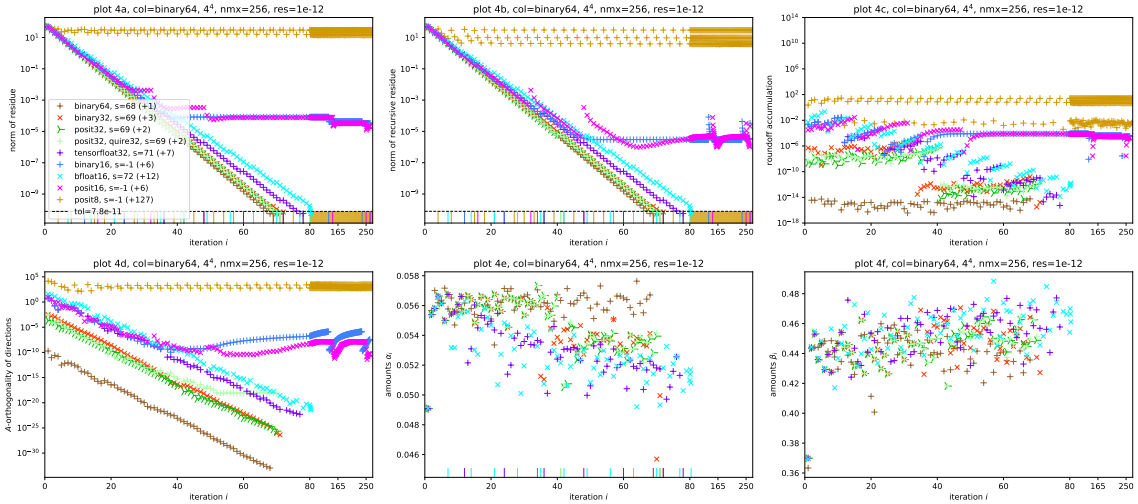

Figure 9: The configuration in these 4 plots is equal to figure 8, besides the value of `res` - the desired relative residue of the calculated solution - is set to 10^{-12} instead of 10^{-6}. Only the 32- and 64-bit number formats converged and gave a meaningful result. Notice that 10^{-12} is outside the representable number range of binary16, posit16 and posit8.

8.5.1 Discussion of figures 6 - 9

Figures 6, 7, 8 and 9 contain all relevant data. It is expected in general that the plots shows datatypes of the same bit-length in clusters and exhibits a hierarchy in precision and exponent range; more precision and larger exponent range should end up in faster convergence. Thus we expect the following hierarchy (where smaller means convergence in fewer steps)

$$\text{binary64} < \text{posit32} \leq \text{binary32} \leq \text{tensorfloat32} \leq (1) \leq \text{posit16} \leq \text{binary16} \leq (2) < \text{posit8}, \quad (8.2)$$

where bfloat16 could be either at position (1) or (2), depending on what is more important; precision or number range.

In the *first row* where the datatype is naively replaced by the simulated datatype, it can be concluded that only datatypes with large enough number ranges converged. binary64, binary32 and posit32 converged each after `status=34` steps. The less precise tensorfloat32 took `status=35` and the even less precise bfloat16 needed `status=56` steps. Such a hierarchical result was expected since they have the same exponent range and thus approximately the same number range, but differ in precision (see table 1). Notice that the less precise the datatype, the more reset steps are needed. This happens because the precision limit of the simulated datatype is reached faster, it the datatype has less precision.

The roundoff accumulation error of posit32 is slightly better than the one of binary32, although defeated by 8 orders of magnitude of binary64 because of its much more precision. It is notable to remark that the roundoff accumulation does not increase substantially from step to step, what would be expected from a recursive calculation. The reason for the small difference between binary32 and posit32 could be that the involved real numbers are closer to representable numbers in posit32 than in binary32. Posits have a larger number density around 1 compared to floats of the same bit-length, and therefore more precision in that regime (see figure 4 for the example of binary16 versus posit16). Posits also have more numbers, because they have no NaNs. Roundoff accumulation is specially dependent on the precision of the datatype, which makes sense; the lower the precision, the higher the roundoff accumulation. The difference in A-orthogonality is neglectible for posit32 compared to binary32, but again clearly surpassed by binary64.

binary16 did not converge (`status=-1`) after the maximal number of `nmx=256` steps. Its footprint is absent in plot *1d*, because it consisted only of NaNs and infinities, causing $\alpha_i = 0$ and $\beta_i = 1$. This implied that $\vec{r}_i = \vec{r}_{i+1}$ and $\vec{d}_{i+1} = \vec{r}_{i+1}$ and therfore $\vec{x}_{i+1} = \vec{x}_i$ and the algorithm stalled. This explains the residues not changing in plots *1a* and *1b*. The reason for the first infinity was an overflow when calculating the norm of $\vec{b}$ in the very first iteration. This suggests that the very limited number range of binary16 might not be enough (at least for a naive replacement), comparing to bfloat16 with the same bit-length, but larger number range that was able to converge, although very slowly.

The behavior of posit8 is very similar to binary16, but without the overflow, because posit do not overflow by definition. Instead the biggest representable number is returned or in case of an underflow the smallest representable number is returned [4]. The algorithm stalled at a value of the norm of the recusive residual of $\|\vec{r}_i\| = 8$. The biggest 8-bit posit number with exponent bits $es = 0$ is $2^6 = 64$, so the norm squared cannot be bigger than 64 and the norm itself cannot be bigger than $8 = \sqrt{64}$ (see plot *1b*). This happend in the first step, whereas the actual residual in binary64 was $\backsim 10^3$. The amounts $|\alpha_i| \ll 1$ in iterative steps are therfore very small causing $\vec{x}_{i+1} \approx \vec{x}_i$. Significant changes in $\vec{x}_i$ will not happen and convergence is unlikely. Also notice that posit8 had 256 reset steps, which means that after every step there was a reset step. The steps where caused by the very high precision limit of posit8. The value of `PRECISION_LIMIT` is `100*MACHINE_EPSILON`, which has a value of 3.125 for posit8.

The story of posit16 is very similar, just that the maximal representable value with $es = 1$ is 268,435,456 and the square root of this is 16,384 which is reached after 8 steps (see plot *1b*). The actual residual in the 8-th step was $\backsim 10^7$, the algorithm diverged and then stalled. Iterative steps are therfore mostly too small and convergence is unlikely.

We observe that number range is more important than precision, when naively replacing the datatype, but the higher the precision, the faster the convergence and the less reset steps needed.

In the *second row* the replacement utilised the possibility to use quires for the posit runs. Therefore, the numbers for the float datatypes are exactly equal to the ones in the first row, because floats have no such feature. They are not discussed again.

Comparing plots *1c* and *2c* and looking at posit32, one can see that the roundoff accumulation in the residual due to its recursive calculation is slightly better than without using the quire. This makes sense, because quires introduce deferred rounding. This is exploited specially in the calculation of norms and matrix-vector products. It also results in a somewhat better maintaining of A-orthogonality for the direction vectors.

However, the data points of posit16 bear little resemblance to its previous or later runs. It comes much closer to the target residual tolerance than in the last simulation, but it is still not reached. The tolerance is within the number range of posit16, even so it did not converge. The reason for this is that the smallest number representable in posit16 is 2^{-28}. The quire for posit16 has the same number range, despite the 128 bits in length. Every norm squared of a non-zero vector must be larger to equal to this number, because posit do not underflow. Therefore the norm is always larger or equal to $\sqrt{2^{-28}} = 2^{-14} \approx 6.1 \cdot 10^{-5}$. The tolerance of $7.8 \cdot 10^{-5}$ - even though larger than that number - is perhaps still too close. Comparing the lightpink values, that are posit16 as well, but the relative residual `res` is set to 10^{-5} instead (the tolerance being one order of magnitude larger), they converged after only `status=31` steps. This suggests that the reason for the strange behavior lies in the relative residual that was chosen too close to the lowest number above zero of the number regime.

Using the same arguments and analysis, posit8 had no chance to give a meaningful result.

In figure 8, a smarter replacement was done. All variables that have a colletive role suffer from overflow. For example the norm of a vector $\vec{v} \in \mathbb{R}^n$ is

$$\|\vec{v}\| = \sqrt{\sum_{i=1}^{n} v_i^2}.$$

The number below the square root may be much bigger before squaring than after. If we calculate the norm in posit8, the result will be $\|\vec{y}\| \leq 8$. More importantly, when using a datatype that overflows such as binary16, the value after squaring might be perfectly fine, but the value under the square root could be outside the range of representable numbers, $\sqrt{\infty} = \infty$ and $\sqrt{0} = 0$. This is cured if the collective variable is of a datatype with bigger range than the underlying datatype that is summed over. In figure 8 all collective variables were of type binary64.

The data of binary64 exhibits no significant alterations. Again comparing binary32 and posit32 with their previous data points, we see that the roundoff accumulation of binary32 is a little better and posit32 is approximately the same as with the quire, suggesting that when using posits utilizing the quire is probably sufficient.

Looking at tensorfloat32, it has the same exponent range as binary32, but less precision and it has the same number of mantissa bits as binary16, but at a higher exponent range. Compared to binary16, both datatypes have the same amount of numbers to be distributed in their respective number range. It is expected to perform worse or equal to binary32, but better or equal to binary16 and bfloat16. Therefore it's expected to converge in $34 \leq$ `status` ≤ 35 steps, see equation (8.2). This is indeed the case with `status=35` steps. We see that the larger number range compared to binary16 has little to do with speed of convergence. This is because the number regime is within the binary16 regime, except for collective variables. This explans as well why tensorfloat32 performed precisely as in the first row, but the roundoff accumulation is better because of the more precise collective variables.

The bfloat16 with even less precision but comparable number range of tensorfloat32 converged in `status=35` steps as well, but needed one more reset step, tightening the previous conclusion about speed of convergence.

The most interesting data points are the ones of binary16 and posit16 that both were able to converge in `status=35` and `status=40` steps respectively. They performed quite similar, even though it would be expected that posit16 would perform a slightly better because of the bigger number range and bigger number density in relevant number regimes (see figure 4). In plot *3c* the increase of roundoff accumulation can be observed for binary16 and posit16 in steps where the real residue changes (where the algorithm makes progress, see for example: steps 1 to 15). Notice that, when the real residue stalls and the recusive residue still (wrongly) decreases, the roundoff accumulation will saturate until the order of magnitude of the two numbers becomes too large such that their difference is dominated by the larger number. This can the seen in the data points of posit16 in plot *3a*. It

suggests that the precision limit was chosen too low for the datatype. Notice that the precision limit is defined to be 100 times the `MACHINE_EPSILON` of the datatype. The `MACHINE_EPSILON` for the posit datatypes is quite misleading, because it gives us (by definition) the precision of numbers around 1. This is the regime where posits are most precise, their precision falling off very rapidly when leaving it. Thus for posit16 in the regime 10^{-1} the `MACHINE_EPSILON` is correct (seen at iteration 16), whereas in the regime 10^{-3} it is chosen to small and we can see a staircase-shape around the reset steps at iterations 32 and 41. Such a stalling of the real residue should be avoided at any cost, because the algorithm stalls as well in that case. The `MACHINE_EPSILON` is defined to be the difference between 1 and the lowest number above 1. For floats this definition makes more sense, because their precision does not fall off that fast, but for posits which are most presice around 1 this gives a too precise value, not refecting the real precision of posits in their whole number range correctly. Instead, the machine epsilon should be a function of the number regime, increasing when going far away from 1. This is the reason for the staircase-shaped curve of posit16 in plot *3a*. The phenomenon is even more prominent for posit16 in plot *4a*. The posit32 does not have this problem, because its `MACHINE_EPSILON` is sufficient for the number regime used in the algorithm.

Comparing binary16 with bfloat16 and tensorfloat32, we see again that exponent range is less relevant than precision. Presicion determines the amount of reset steps.

The *fourth row* shows all the simulated datatypes using a collective datatype of binary64 just as in the third row, but with a relative resudial of 10^{-12} instead. This might be a more realistic scenario. The last row resembles the predicted hierarchy (8.2) particularly well. Notice that 10^{-12} is outside the representable number range of binary16, posit16 and posit8. This means that these datatypes have no chance to reach the target tolerance, therefore we expected them not to converge. This is indeed the case. We also see that binary16 and posit16 both are not able to go below 10^{-5}, meaning the tolerance in the third row was chosen very close to the minimum possible, but still converging tolerance (see also discussion of posit16 in the second row). Both datatypes make no further significant progress after step 45. It can also be seen that even the recusive residue stalls or increases - an indicator that the datatype has reached its limits.

The comparison between binary32 and posit32 is again of insight. Their difference is subtile. We see that both needed the same amount of steps, but binary32 required one reset step more than posit32. Roundoff accumulation and A-orthogonality are again slightly better, making posit32 the overall better 32-bit datatype for the problem. The reason for this goes down to the higher precision of posits in the relevant number regime. Looking at the lightgreen values, that are posit32 as well, but utilizing the quire instead of binary64 as collective variable, we observe the same amount of steps to convergence, but roundoff accumulation is slighly worse. It might be an unfair comparison, because binary64 as collective variable has more precision, surpassing even the deferred rounding employed by the 512-bit quire for posit32. In plot *4d* the posit32 with quire will not go below some fixed value. The reason for this is the lowest posit32 value with exponent bits `es=2` is 8^{-30} and the norm of a posit32-vector with at least one non-zero component must be bigger or equal to the square root of this; $1.15 \cdot 10^{-18}$. This suggests that when choosing `res` to be smaller than 10^{-18}, we expect posit32 not to converge anymore in analogy to posit16 in the second row.

Since binary16 was able to converge in the third row, this suggests that the number regime is within binary16 giving posit32 more precision in that regime over binary32

Finally, compare the 3 datatypes with the same exponent range, but different precisions; binary32, tensorfloat32 and bfloat16. The less precision, the slower the convergence. The price to go from 23 to 10 mantissa bits results in 2 more conjugate gradient steps as well as 4 more reset steps. When going further down to 7 mantissa bits again 1 more regular step and 5 more reset steps where needed to finally bring bfloat16 to convergence after `status=72` regular conjugate gradient plus 12 reset steps. Bearing in mind that it uses only 16 bits, this is a remarkable result. It performed way better than its 16-bit competitors.

We also see in plot *4a* that all datatypes start to converge by the same speed (all slopes are equal). The actual residual of the datatype with the lowest precision, namely bfloat16 with 7 mantissa bits, resets first, followed by binary16 and tensorfloat32 which have both 10 mantissa bits. The next one is posit16, because it has more precision than binary16 in the relevant regime, followed by binary32 with 23 mantissa bits and later by posit32, where the same argument as before holds. The curve of binary64 would also reset at some point, but that is outside the scale.

Specially plot *4a* suggests that we can start to calculate in a datatype with 16 bits of length until we fall below a constant, to be determined value (that depends on the datatype), then continuing the

calculation in a datatype with 32 bitlength until that number regime is exhausted, again switching to a 64 bit datatype to finish the caclulation.

8.5.2 8^4 lattice

In order to make sure that the previous analysis is consistent and the physics involved were relevant, the same data was extracted from a 8^4 lattice and some of the plots were remade from the new data, see figure 10. Only the datatypes binary64, binary32 and binary16 were simulated. In priciple, the data tells the same story. The main difference to figures 8 and 9 is that more steps were needed to converge, because the Dirac matrix is much larger than before, although only 0.04% of all components were non-zero, compared to 2% in the 4^4 lattice of the previous analysis. In the *second row*, were the relative residue was chosen to be 10^{-12}, we again see the saturation of binary16 marking the lower limit of the datatype. After every reset step, a jump in roundoff accumulation can be seen, because the residual in the reset step is calculated in higher precision. It is interesting that the roundoff accumulation in the final steps of binary16 come very close to those of binary32 (see plot *1c*). A reason for this could be the clustering of reset steps just before convergence, giving very accurate results with little roundoff, even for less presice datatype. We also see that the speed of convergence does not significantly depend on the precision of the datatype, only the amount of reset step does, thus the less steep slope of binary16. When the lower limit of the datatype is reached, the slope becomes zero and the residual shows no striking reduction anymore. This is were the datatype should be switched to one with a larger number range.

8.5.3 Conclusion

The desicion between floats and posits is not trivial. It highly depends on how fast the machine can perform FLOPS and POPS. For example division in floating point arithmetic is very expensive (it may exceed 24 CPU cycles, many compiler optimizations evade them), whereas in posit arithmetic it is said to be cheap, because obtaining the inverse of a number is easy.

Another example could be that comparisons between floats are more expensive than for posits. Two posits are equal if their bit representations are equal. Comparing two floats is much more expensive, mainly because of the many NaNs and since 0 and -0 are equal but not bit-identical.

On the other hand, there is currently no hardware available, that has dedicated posit units and posits are not studied as intensive as floats. Floats are widespread, well understood and implemented in common hardware.

If one desides to replace binary32 with posits, the most elegant solution would be to naively replace the datatype and utilize quires in collective operations. To use binary64 collective variables is not recommended, because this would introduce many type conversions between the floating point and the posit format which is assumed to be expensive. The drawback ot this method is that posit16 may only converge if the relative residue is chosen high enough (see plot *2a* in figure 7).

If the desicion goes for floats, which might be the more realistic scenario, then the most elegant solution would be to use collective variables in binary64. Type conversions between different IEEE floating point types are not considered to be expensive. The tensorfloat32 compared to binary32 and bfloat16 answers the question how important precision is in the calculation. All of them have the same number of exponent bits and therefore approximately the same number range, but very different precisions. We see that all of them were able to converge in any experiment, but with binary64 as collective variable, the results were closest to each other (see figure 8 plot *3a*). The only real difference was in the amount of reset steps. If the datatype is lower in bitlength, the memory-boundedness suggests that the calculation performs faster, but the tradeoff is the amount of (computationally expensive) reset steps that increases with less precision. However, the datatype for collective operations should be precise and should have a large number range. Since the amount of variables needed in that datatype does not scale with the lattce size, it is perfectly right to use a datatype with large bitlength. Comparing the convergence of bfloat16 in the naive case (figure 6 plot *1a*) with the case binary64 collective variables (figure 8 plot *3a*), it can be seen that the algorithm converged 21 steps faster, only because the collective datatype was chosen to be binary64. On the other hand, comparing the performance of binary16 in the two plots, we see that the number range of the collective datatype brought binary16 from no convergence to convergence within `status=35` steps - only marginally slower than binary32. These arguments make binary64 the best choice for variables with a collective role.

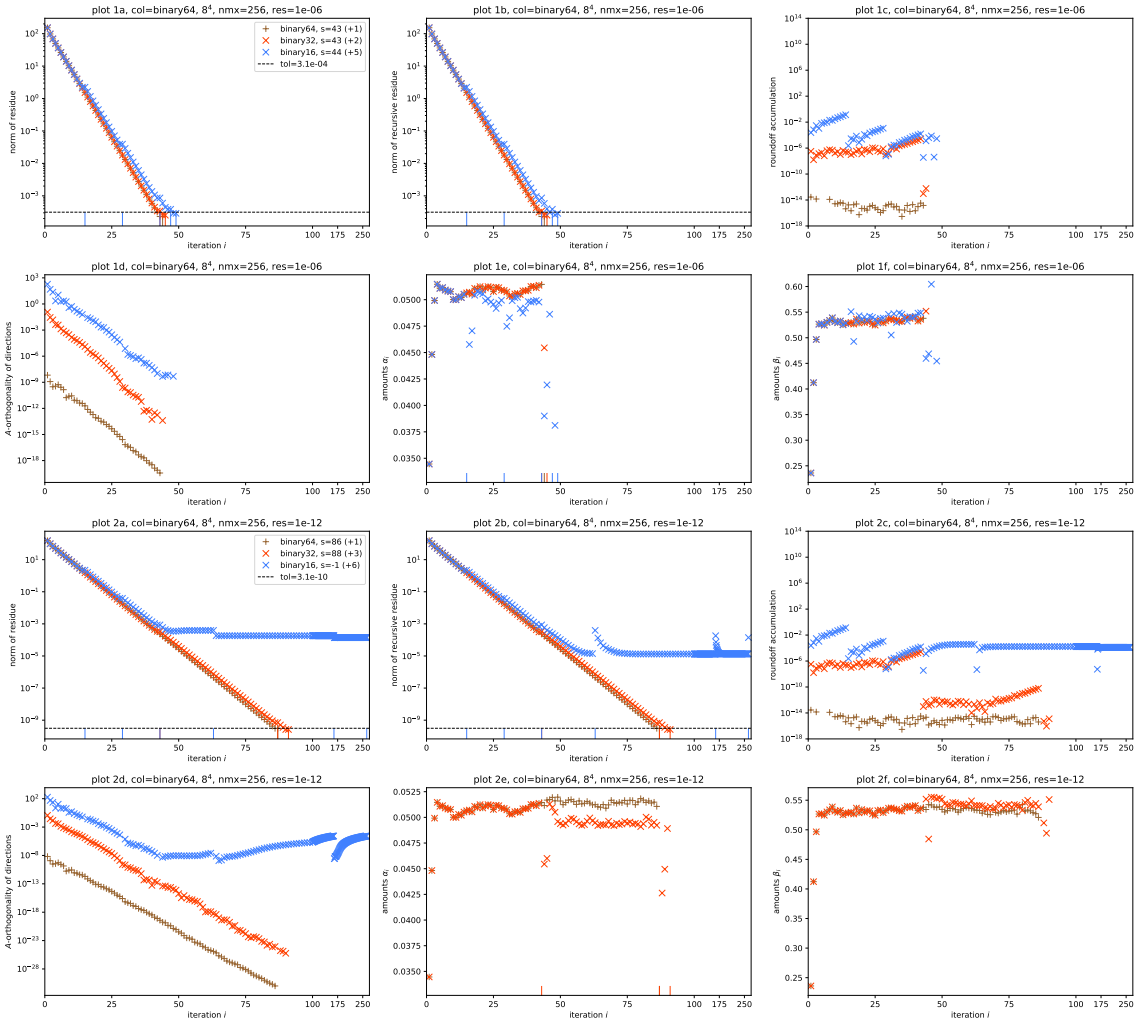

Figure 10: In anology to figures 8 and 9. This time an 8^4 lattice was used and only the floating point datatypes that are available in hardware nowadays were simulated. The *first and second row* use binary64 as collective variable and 10^{-6} was the desired relative residual. The *third and fourth row* have the exact same setup, but with a relative residual of 10^{-12} instead.

Proposal 8.1 (mixed precision). TODO: proposal for mixed precision conjugate gradient or other algorithms.

Proposal 8.2 (approximating the amounts α_i). TODO: proposal approx. the alphas

res $> 10^{-6}$
Simulated datatype: precision > number range
Collective datatype: number range > precision
res $< 10^{-6}$
Simulated datatype: precision > number range
Collective datatype: number range > precision

9 Summary

TODO

10 References

[1] I. Buck. Taking the plunge into gpu computing. *GPU Gems*, 2:509–519, 2005.

[2] I. Campos, P. Fritzsch, M. Hansen, M. Krstić Marinković, A. Patella, A. Ramos, and N. Tantalo. openq*d. https://gitlab.com/rcstar/openQxD, 2018. Accessed: 2021-01-06.

[3] W. Cody. Towards sensible floating-point arithmetic. Technical report, Argonne National Lab., IL (USA), 1980.

[4] P. W. Group et al. Posit standard documentation - release 3.2-draft. *Posit Standard Documentation*, 2018.

[5] J. L. Gustafson. Posit arithmetic. *Mathematica Notebook describing the posit number system*, 30, 2017.

[6] J. L. Gustafson and I. T. Yonemoto. Beating floating point at its own game: Posit arithmetic. *Supercomputing Frontiers and Innovations*, 4(2):71–86, 2017.

[7] R. Krashinsky, O. Giroux, S. Jones, N. Stam, and S. Ramaswamy. Nvidia ampere architecture in-depth. *NVIDIA blog: https://devblogs. nvidia. com/nvidia-ampere-architecture-in-depth*, 2020.

[8] I. of Electrical, E. E. C. S. S. Committee, and D. Stevenson. *IEEE standard for binary floating-point arithmetic*. IEEE, 1985.

[9] I. of Electrical, E. E. C. S. S. Committee, and D. Stevenson. *IEEE standard for binary floating-point arithmetic*. IEEE, 2008.

[10] R. G. T. REMOVE. Github repository: Source code of the implementation. http://github.com/chaoos/TODO, 2021. Accessed: 2021-01-01.

[11] J. R. Shewchuk et al. An introduction to the conjugate gradient method without the agonizing pain, 1994.

[12] S. Wang and P. Kanwar. Bfloat16: the secret to high performance on cloud tpus. *Google Cloud Blog*, 2019.

Appendices

A Code

All code used in this report is open source and can be found in the GitHub repository [10]

Acronyms

BLAS Basic Linear Algebra Subprograms. 9

FLOPS Floating Point Operations Per Second. 23

MPI Message Passing Interface. 27

NaN not a number. 11, 13, 20, 23

POPS Posit Operations Per Second. 23

QCD Quantum chromodynamics. 2

Glossary

bfloat16 Googles Brain float [12] floating point number representation with encoding in length of 16 bits. 11, 12, 15, 17, 20–23

binary16 IEEE754 2008 [9] conformant floating point number representation with encoding in length of 16 bits. 11, 12, 14–17, 19–23

binary32 IEEE754 2008 [9] conformant floating point number representation with encoding in length of 32 bits. 10–12, 15–18, 20–23

binary64 IEEE754 2008 [9] conformant floating point number representation with encoding in length of 64 bits. 10–12, 16–24

fused multiply–add A multiply-add operation $a + bc$ in one shot, where the rounding is deferred. 14

posit16 Posit Standard [4] conformant storage format for real number representation with encoding in length of 16 bits and an exponent size of `es=1`. 14, 15, 17, 19–23

posit32 Posit Standard [4] conformant storage format for real number representation with encoding in length of 32 bits and an exponent size of `es=2`. 14, 15, 17, 20–22

posit64 Posit Standard [4] conformant storage format for real number representation with encoding in length of 64 bits and an exponent size of `es=3`. 14

posit8 Posit Standard [4] conformant storage format for real number representation with encoding in length of 8 bits and an exponent size of `es=0`. 14, 17, 19–22

quire Posit Standard [4] conformant special fixed-size data type that can be thought of as a dedicated register that permits dot products, sums, and other operations to be performed with rounding error deferred to the very end of the calculation [5]. 14, 18–23

rank In MPI a process is identified by its rank, with is an integer between $[0, N-1]$, where N is the size of the MPI process group. 2

sparse matrix A matrix, where most of the entries are 0. 2

tensorfloat32 Nvidias TensorFloat-32 [7] floating point number representation with encoding in length of 32 bits, but only 19 bits are used. 11, 12, 15, 17, 20–23